

Published in final edited form as:

Nanomedicine. 2011 October ; 7(5): 580–587. doi:10.1016/j.nano.2011.01.011.

Mechanism of Anti-angiogenic Property of Gold Nanoparticles: Role of Nanoparticle Size and Surface Charge

Rochelle R. Arvizo, Ph.D¹, Subinoy Rana, M.Sc², Oscar R. Miranda, Ph.D², Resham Bhattacharya, Ph.D¹, Vincent M. Rotello, Ph.D^{2,*}, and Priyabrata Mukherjee, Ph.D^{1,3,4}

¹ Department of Biochemistry and Molecular Biology, Mayo Clinic College of Medicine, Rochester, MN 55905

² Department of Chemistry, University of Massachusetts, Amherst, MA 01003

³ Department of Physiology and Biomedical Engineering, Mayo Clinic College of Medicine, Rochester, MN 55905

⁴ Mayo Clinic Cancer Center, Mayo Clinic College of Medicine, Rochester, MN 55905

Abstract

Discovering therapeutic inorganic nanoparticles is evolving as an important area of research in the emerging field of nanomedicine. Recently, we reported the anti-angiogenic property of gold nanoparticles (GNPs): it inhibits the function of pro-angiogenic heparin-binding growth factors (HB-GFs) such as vascular endothelial growth factor 165 (VEGF165), basic fibroblast growth factor (bFGF), etc. However, the mechanism through which GNP imparts such an effect remains to be investigated. Using GNPs of different sizes and surface charges we demonstrate here that a naked GNP surface is required and core size plays an important role to inhibit the function of HB-GFs and subsequent intracellular signaling events. We also demonstrate that the inhibitory effect of GNPs is due to the change in HB-GFs conformation/configuration (denaturation) by the nanoparticles, whereas the conformations of non-HB-GFs remain unaffected. Significantly, this study will help structure-based design of therapeutic nanoparticles to inhibit the functions of disease causing proteins.

Keywords

Gold nanoparticles; Angiogenesis; VEGF165; Protein conformation

Introduction

It is recognized that angiogenesis plays a pivotal role in pathological diseases such as age related macular degeneration, arthritis, ischemic heart disease, tumorigenesis, and metastasis [1]. This neovascular development from preexisting vessels is essential for the growth and progression of tumors [2, 3] in which vascular endothelial growth factor (VEGF) has been recognized as the prominent cytokine in the angiogenic cascade [4]. VEGF 165, the most

© 2011 Elsevier Inc. All rights reserved.

*Address for Correspondence: Priyabrata Mukherjee, PhD, Department of Biochemistry and Molecular Biology, Gugg 1321B, College of Medicine, Mayo Clinic, 200 First St SW, Rochester, MN 55905, Mukherjee.priyabrata@mayo.edu.

Publisher's Disclaimer: This is a PDF file of an unedited manuscript that has been accepted for publication. As a service to our customers we are providing this early version of the manuscript. The manuscript will undergo copyediting, typesetting, and review of the resulting proof before it is published in its final citable form. Please note that during the production process errors may be discovered which could affect the content, and all legal disclaimers that apply to the journal pertain.

portent among its several isoforms, is a heparin binding protein [5]. The binding of VEGF 165 with its tyrosine kinase receptor KDR (aka VEGFR-2), initiates a number of signaling cascades, end point of which is the proliferation of endo-thelial cells leading to migration and angiogenesis. Hence, therapeutic antibodies against VEGF165 have been developed and currently used in the clinics to inhibit VEGF165 function [6]. However, use of the anti-angiogenic therapy lead to some serious and unexpected toxicities of anti-VEGF antibodies treatment [6]. Moreover, it is recognized that due to tumor heterogeneity blocking a single pathway is not ideal therapeutic option for long term patient care. Thus, developing a new class of anti-angiogenic agents that will simultaneously inhibit the function of multiple growth factors might be important to overcome such a problem. Hence, GNPs might be interesting in this aspect as it not only blocks the function of VEGF165 but also other HB-GFs such as bFGF, PIGF, etc.

Discovering therapeutic inorganic nanoparticles is evolving as an important area of research in the emerging field of nanomedicine [7–12]. Some biologically occurring biomolecules can act as an antiangiogenic agent such as PolyP [13]. Other inorganic nanoparticles have also been shown to abrogate VEGF 165 in ocular disease [14]. Gold and silver nanoparticles, in particular, have also demonstrated some promising outcome [15–20]. Furthermore, gold nanoparticles have generated significant interest in various biomedical applications including detection, diagnosis and therapy due to their relatively favorable safety profile and ease of surface functionalization [21–23]. Recently, we reported that naked GNPs can inhibit the function of pro-angiogenic heparin-binding growth factors such as vascular endothelial growth factor 165, basic fibroblast growth factor and PIGF [24]. However, the mechanism of such anti-angiogenic property of gold nanoparticles is not clear. Determining the mechanism of such inhibitory effect is essential for future clinical translation of inorganic nanoparticles-based anti-angiogenic agents. These inorganic anti-angiogenic agents may overcome the unusual toxicities associated with the traditional anti-angiogenic agents presently used in the clinic. Thus, to determine the mechanism of anti-angiogenic property of GNPs we investigated the role of nanoparticle core size, surface charge and their ability to change the conformation of HB-GFs and non-HB-GFs. Furthermore, modifying the surface functionality may allow for specific interactions with biomacromolecules through favorable electrostatic or lipophilic interactions [25, 26]. Using GNPs of different sizes and surface charges we demonstrate here that a naked GNP surface is required and core size plays an important role to inhibit the function of HB-GFs (VEGF165; bFGF) and subsequent intracellular signaling events. We also demonstrate that the inhibitory effect of GNPs is due to the change in HB-GFs conformation/configuration (denaturation) by the nanoparticles, whereas the conformations of non-HB-GFs remain unaffected. Significantly, this study will help structure-based design of therapeutic nanoparticles to inhibit the functions of disease causing proteins.

Materials and methods

Gold nanoparticles

The 5, 10, and 20 nm citrate reduced nanoparticles were purchased from Ted Pella (Redding, Ca). They were used without any modifications (Supplemental Figure 4). Media and PBS was purchased from Mediatech (Manassas, VA) unless otherwise noted. Positively charged gold nanoparticles were synthesized according to reported procedures [27].

Zeta potential and size measurements

ζ -Potential (ZP) and dynamic light scattering (DLS) results were used to characterize the charge and the hydrodynamic diameter of both nanoparticles and proteins. The nanoparticles

were dissolved in sodium phosphate buffer (5 mM, pH 7.4) to make solutions of 5 μM concentrations. The samples were filtered through a Millipore syringe filter (0.22 μm) and injected into a folded capillary disposable cell. Both ZP and DLS were measured on a MALVERN Zetasizer Nano ZS instrument. Each sample was scanned six times and an average value was reported.

Cell cultures

Human umbilical vein endothelial cells (HUVECs) were grown on plates coated with collagen and cultured with EGM-MV BulletKit (5% fetal bovine serum in endothelial basal medium with 12 $\mu\text{g}/\text{ml}$ bovine brain extract, 1 $\mu\text{g}/\text{ml}$ hydrocortisone, 1 $\mu\text{l}/\text{ml}$ GA-1000, and human EGF). NIH3T3 were cultured in DMEM media. Experiments were performed in cells at ~80% confluence.

Intracellular Ca^{2+} Release

Serum-starved HUVECs were washed twice with PBS and incubated with 4 ml of collagenase solution (0.2 $\mu\text{g}/\text{ml}$ collagenase, 0.2 $\mu\text{g}/\text{ml}$ soybean trypsin inhibitor, 1 $\mu\text{g}/\text{ml}$ bovine serum albumin, and 2 mM EDTA in PBS) at 37°C for 30 min. Cells were detached by gentle scraping and centrifuged at 1100 rpm for 3 min. Cell pellets were washed twice with PBS and were resuspended in 10 ml of Ca^{2+} buffer and centrifuged at 1000 rpm for 10 minutes. Cell pellets were resuspended in 10 ml of Ca^{2+} buffer containing 1 $\mu\text{g}/\text{ml}$ Fura-2 and 0.02% Pluronic F-127 and incubated at 37°C for 0.5 h. Cells were collected by centrifugation at 1000 rpm for 10 min and re-suspended in 10 ml of Ca^{2+} buffer. Intracellular Ca^{2+} concentrations were measured with the DeltaScan Illumination System (Photon Technology International) using Felix software.

^3H -Thymidine incorporation assay for cellular proliferation

Cells (2×10^4) were seeded in 24-well culture plates in their respective medium. After culturing overnight, they were treated with 10 ng/ml VEGF165 that was preincubated with and without gold nanoparticles (conc = 1 nmol/L) for 24 hours at 4°C. After being cultured with the nano-particle/VEGF 165 mixture, thymidine incorporation assay was performed as previously published [28]. In brief, after 24h, 1 $\mu\text{Ci}/\text{ml}$ [^3H]thymidine was added, and 4h later, cells washed with ice-cold PBS, fixed with 100% cold methanol, washed again, and lysed with 250 μl 0.1N NaOH. [^3H]thymidine incorporation was measured in scintillation solution.

Western Blot Analysis

HUVEC cells were serum starved overnight and stimulated with AuNPs (5, 10, 20nm) preincubated with 10 ng/mL VEGF165. After 5 minutes, stimulation was halted by the addition of chilled PBS, washed thrice in cold PBS, and lysed using RIPA buffer. Cell lysates were centrifuged at 14,000 x g for 10 minutes at 4°C and the supernatant was collected for protein analysis. The supernatant was re-suspended in 2x SDS sample buffer for Western blot analysis. All experiments were repeated at least three times. The primary antibody used was from Santa Cruz (SC-504) in a 1:250 dilution. The secondary antibody dilution was a 1:1000 (anti-rabbit).

Results

Inhibition of HB-GFs induced cell proliferation is dependent on the size of gold nanoparticles

To determine whether the size of nanoparticles plays any role to inhibit the function of HB-GFs, we used commercially available citrate reduced GNPs of 5, 10 and 20 nm (diameter) to

test their ability to inhibit VEGF165 and bFGF induced proliferation of HUVECs and NIH3T3 cells, respectively. VEGF165 and bFGF was first pre-incubated overnight at 4°C with GNPs of different sizes (5, 10, and 20 nm) and then added to serum-starved HUVECs and NIH3T3 cells, respectively. It is evident from the [3H]-thymidine incorporation assay (Figure 1) that VEGF 165-induced proliferation of HU-VECs was significantly inhibited by all sizes of GNPs tested in a concentration dependent manner. The larger nanoparticles (20 nm diameter) showed maximum effect (Figure 1A). The 5 nm GNP exhibited a modest ~25% inhibition of proliferation at 1nmol/L and complete inhibition at 10 nmol/L (Figure 1B). The 10 nm GNP showed ~60% inhibition of proliferation at 1nmol/L and 100% inhibition at 5 nmol/L (Figure 1C). However, complete inhibition of VEGF165-induced proliferation was achieved with 1 nmol/L of 20 nm GNPs (Figure 1D). Similar results were observed with bFGF -induced proliferation of NIH3T3 fibroblast (Figure 2A). Similarly as VEGF165, the 20 nm GNP maximally inhibited bFGF-induced proliferation of NIH3T3 cells as compared to 5 and 10 nm GNPs. However, these particles did not inhibit the activity of EGF, a non-HB-GFs (Figure 2B). These results demonstrate that the specific inhibitory effects of GNPs towards HB-GFs are size dependent, bigger nanoparticles being more efficacious.

GNPs abrogate VEGF165- induced KDR-phosphorylation in a size dependent manner

The angiogenic cascade is initiated when VEGF165 binds to its extracellular receptor, mainly KDR on endothelial cells, leading to receptor phosphorylation and commencing further downstream signaling events [29]. Thus, to confirm whether the inhibition of proliferation of HUVECs is due to the inhibition of VEGF165 function by GNPs of different sizes, we looked at the VEGF165 induced phosphorylation of KDR after pre-incubating VEGF165 with GNPs of different sizes. When VEGF165 was pre-incubated with 5 nm GNPs at a concentration of 1 nmol/L, significant inhibition of KDR phosphorylation was observed (~65 %), whereas complete inhibition was observed with the 20 nm GNPs at the same concentration (Figure 3). The effect of core size on the inhibition of phosphorylation of KDR was also seen to be concentration dependent. The 5 nm GNP showed significant inhibition of KDR phosphorylation at 5 nmol/L and complete inhibition at 10 nmol/L (Sup Fig 1A), whereas the 10 nm GNP showed a modest inhibition at 0.5nmol/L and complete at 1nmol/L (Sup Fig1B). These results indicate that the core size of GNPs plays important role in inhibiting VEGF165 function. Furthermore, it also indicates that GNPs directly bind to VEGF to inhibit its function,

Effect of nanoparticles size and surface charge to inhibit VEGF function

If direct binding of VEGF165 to gold nanoparticles is the cause of inhibition of its activity as evidenced from the KDR-phosphorylation experiments, it is then expected that all of the subsequent downstream signaling events will also be inhibited. To further confirm this, we performed a VEGF165-induced intracellular Ca^{2+} release assay using HUVECs. It is well documented that, HUVECs when stimulated with VEGF165, increase cytosolic $Ca_{[i]}$ released from the endoplasmic reticulum [30]. When VEGF165 was pre-incubated with a concentration of 1 nmol/L of the 5 nm GNP, a modest decrease in Ca^{2+} release was observed, whereas complete inhibition was evident with the 10 nm and 20 nm GNPs at the same concentration (Figure 4a). The effect of core size on VEGF165 induced Ca^{+2} release was also shown to be concentration dependent (Supplemental Figure 2A–C).

Previously we described that the HBD of VEGF plays an important role to interact with nanogold through its $-NH_2$ or $-SH$ functionalities probably via a coordination interaction [31]. All the citrate capped gold nanoparticles have a net negative surface charge of ~ -40 mV. Thus, to investigate whether the electrostatic interaction between the negatively charged GNP and the highly basic HB-domains of VEGF165 plays any role in inhibiting

VEGF function, we used thiolated tetraethylene glycol (NP1-4) functionalized gold nanoparticles with various surface charges (Figure 4B). The use of TEG masks the gold surface [32] thus allowing us to determine the role of surface charge, if any, to inhibit the function of VEGF165. As seen in Figure 4C, when VEGF165 was pre-incubated with NP1-4, no inhibition of VEGF165 induced Ca^{2+} release was observed, even with increasing concentrations of the nanoparticles (Supplemental Figure 3). These experiments clearly demonstrate that the bare gold surface is important and essential to inhibit the function of VEGF165.

Ability of GNP of different sizes to bind VEGF 165

Having demonstrated the size of the GNPs surface is directly related to VEGF inhibition, probably through its cysteine and/or lysine residues[31], we then focused on determining the quantity of VEGF165 bound to the surface of GNPs of different sizes. To address this potential interaction between the naked surface of GNPs and VEGF165, we used an ELISA to determine the concentrations of unbound VEGF165 remaining in solution after incubation with GNPs of different sizes (5, 10, and 20 nm). VEGF165 was incubated with the citrate reduced GNPs at different concentrations and then pelleted using ultracentrifugation. The concentration of unbound VEGF165 in the supernatant fractions notably decreased in a size and concentration dependent manner, with 95% of the protein being bound on the surface of 20 nm GNPs at 1nmol/L concentration compared to 80% bound to the 5nm GNPs respectively (Figure 5A). This data further strengthens the fact that the inhibitory effect of GNPs is due to the direct binding with VEGF165, probably leading to the conformational changes in the protein structure.

We further probed whether direct binding causes conformational changes of the proteins leading to inhibiting the function of HB-GFs. We monitored changes in secondary structure of both HB-GFs and non-HB-GFs upon incubation with different sized citrate GNPs using circular dichroism (CD). The far-UV CD spectrum shows dramatic change in the conformation of bFGF in the presence of citrate reduced GNPs. These changes in the protein conformation are reflected by both the shift and increase in intensity of the characteristic minima of native bFGF at 204 nm (Figure 5B). [33, 34] The maxima between 227–229 nm of native bFGF were also changed for all the GNPs and became prominent as the concentration of GNP increased. However the CD spectrum for EGF incubated with GNPs was in good agreement with the spectra of native rhEGF [35], indicating that the secondary structure of non-HB-GF, EGF, was not disrupted by the nanoparticle (Figure 5C). This result demonstrates that GNPs have a significant effect on the structure of HB-GFs that ultimately dictates the protein function.

Discussion

Anti-angiogenic therapy is a viable therapeutic option in cancer. To be successful, the therapeutic should either target multiple angiogenic factors or an angiogenic factor that is critical to angiogenesis or specifically control a host of other angiogenic factors. Bevacizumab, a monoclonal antibody that binds and inactivates VEGF165 effectively inhibits cell signaling and proliferation [36]. Although there is a positive response when Bevacizumab is combined with chemotherapy, there is a question of its tolerability [37]. Patients treated with Bevacizumab had complications due to GI perforations and/or arterial thromboembolism. Since VEGF also regulates normal physiologic processes, such as wound healing and stabilization of damaged endothelia, thus total inhibition of VEGF may create a unique toxicity. Other small molecule inhibitors, such as Sunitinib, have also been developed to inhibit protein tyrosine kinases. The FDA has recently approved this drug for treatment of renal cell carcinoma and gastrointestinal stromal tumors. However, with its

being able to target multiple receptors, Sunitinib has numerous side effects such as hyperthyroidism, hand-foot syndrome, cardiac dysfunction, and brain hemorrhage [38].

Nanoparticles have piqued the interest of the medical community for use in cancer diagnosis, treatment, and as delivery vectors for biologic or pharmacologic agents [39]. The ability to affect diagnostic or therapeutic changes on a nanoscale could provide significant gains in medical care. Metallic gold compounds are widely used in medicine, with the most common being a therapeutic for reducing rheumatoid arthritis symptoms since the early 1900's [40]. With its long history of use in humans, the FDA has recently approved a gold nanoparticle conjugated system for Phase-I clinical trials for the treatment of solid tumors. Along with being biocompatible, gold nano-particles are easily synthesized and readily modified to create a tailored and effective multifunctional drug delivery system. Recent reports using nanogold imply that they can disrupt/inhibit the activity of pro-angiogenic cytokines containing a heparin-binding domain (HBD) such as VEGF165, basic fibroblast growth factor (bFGF), and PIGF ([31]; [41]). The nature of bonding between gold and proteins has been the subject of intense investigation over the last several decades. It is now generally accepted that there are three main types of interactions that occur between a protein/antibody and a gold nano-particle; (i) electrostatic interactions of negatively charged GNPs with positively charged proteins; (ii) covalent interactions between the thiol/amine groups present within amino acid residues in antibodies and the GNPs; and (iii) hydrophobic interactions between proteins and GNPs [28, 42, 43]. Using X-ray photoelectron spectroscopy and thermo-gravimetric analysis we previously demonstrated that cetuximab, VEGF antibody and VEGF165 utilize thiol and amine functionalities to bind to gold nanoparticles [42]. In the present study, we further assess the anti-angiogenic properties of gold nanoparticles with respect to the nanoparticle size and surface charge. By modifying the surface functionality, it allows for specific interactions with biomacromolecules through favorable electrostatic *or* lipophilic interactions [44, 45]. These studies are important to gain further insight into the mechanism of GNP-induced anti-angiogenesis for future therapeutic application. To that end, we demonstrate here using human umbilical vascular endothelial cells (HUVECs) and NIH3T3 fibroblast cells that the naked GNP surface and the core size is important in culling the intrinsic activity of their respective HBD growth factors (VEGF165; bFGF) and subsequent intracellular signaling events.

Since VEGF regulated angiogenesis is known to play a crucial role in many pathological angiogenesis such as cancer, we wanted to further probe the interaction between HB-GFs and GNPs with different size and charge. We chose to use citrate reduced gold nanoparticles since they have been synthesized by well-established method and commercially available. Interestingly GNPs are selective to inhibit the function of HB-GFs whereas non-HB-GFs remain unaffected upon preincubation with GNPs. In this respect, the 20 nm GNP is the most potent among all the 3 sizes tested to inhibit the function of HB-GFs. Furthermore, surface modification of GNPs with different ligands (**NP1-4**) prevents their ability to inhibit the HB-GFs function, clearly emphasizing the role of naked nanoparticles surface.

The data presented here demonstrates that GNPs inhibit the VEGF signaling cascade *in vitro*, which may contribute to disease treatment. The anti-angiogenic mechanism of GNPs is unique and needs to be investigated further. In summary, we investigated the mechanism of anti-angiogenic property of gold nanoparticles. GNPs selectively disrupt the functions of pro-angiogenic HB-GFs in a size dependent manner *in vitro*. Furthermore, surface modification of GNPs with various charged ligands prevents their ability to inhibit the HB-GFs function, clearly emphasizing the role of the naked nanoparticle surface. Circular dichroism confirms that such inhibitory effect is due to the change in conformation of HB-GFs upon binding to GNPs, whereas the conformation of non-HB-GFs remains unaffected.

These findings provide strong evidence to design therapeutic nanoparticles to inhibit the function of disease causing proteins in a structure depended manner.

Supplementary Material

Refer to Web version on PubMed Central for supplementary material.

Acknowledgments

Supported by NIH CA135011, CA136494 and UTMD-1 grants (PM) and GM GM077173 (VMR).

List of abbreviated words

GNP	gold nanoparticles
VEGF 165	vascular endothelial growth factor 165
HB-GFs	heparin-binding growth factors
bFGF	basic Fibroblast Growth Factor
KDR	tyrosine kinase receptor
EGF	endothelial growth factor
HU-VEC	Human umbilical vein endothelial cells

References

- Lee JH, Canny MD, De Erkenez A, et al. A therapeutic aptamer inhibits angiogenesis by specifically targeting the heparin binding domain of VEGF165. *Proc Natl Acad Sci U S A*. 2005; 102(52):18902–7. [PubMed: 16357200]
- Carmeliet P, Jain RK. Angiogenesis in cancer and other diseases. *Nature*. 2000; 407(6801):249–57. [PubMed: 11001068]
- Risau W. Mechanisms of angiogenesis. *Nature*. 1997; 386(6626):671–4. [PubMed: 9109485]
- Nagy JA, Vasile E, Feng D, et al. Vascular permeability factor/vascular endothelial growth factor induces lymphangiogenesis as well as angiogenesis. *J Exp Med*. 2002; 196(11):1497–506. [PubMed: 12461084]
- Ferrara N, Gerber HP, LeCouter J. The biology of VEGF and its receptors. *Nat Med*. 2003; 9(6):669–76. [PubMed: 12778165]
- Ferrara N, Kerbel RS. Angiogenesis as a therapeutic target. *Nature*. 2005; 438(7070):967–74. [PubMed: 16355214]
- Ghosh P, Han G, De M, Kim CK, Rotello VM. Gold nanoparticles in delivery applications. *Advanced Drug Delivery Reviews Inorganic Nanoparticles in Drug Delivery*. 2008; 60(11):1307–1315.
- Christof M, Niemeyer. *Nanoparticles, Proteins, and Nucleic Acids: Biotechnology Meets Materials Science*. *Angewandte Chemie International Edition*. 2001; 40(22):4128–4158.
- De M, You CC, Srivastava S, Rotello VM. Biomimetic interactions of proteins with functionalized nanoparticles: a thermodynamic study. *J Am Chem Soc*. 2007; 129(35):10747–53. [PubMed: 17672456]
- Giljohann D, Seferos D, Daniel W, Massich M, Patel P, Mirkin C. *Gold Nanoparticles for Biology and Medicine*. *Angewandte Chemie International Edition*. 49(19):3280–3294.
- Daniel MC, Astruc D. Gold nanoparticles: assembly, supramolecular chemistry, quantum-size-related properties, and applications toward biology, catalysis, and nanotechnology. *Chem Rev*. 2004; 104(1):293–346. [PubMed: 14719978]
- Pitsillides C, Joe E, Wei X, Anderson R, Lin C. Selective cell targeting with lightabsorbing microparticles and nanoparticles. *Biophysical J*. 2003; 84:4023 – 4032.

13. Han KY, Hong BS, Yoon YJ, et al. Polyphosphate blocks tumour metastasis via anti-angiogenic activity. *Biochem J.* 2007; 406(1):49–55. [PubMed: 17492939]
14. Chen J, Patil S, Seal S, McGinnis JF. Rare earth nanoparticles prevent retinal degeneration induced by intracellular peroxides. *Nat Nanotech.* 2006; 1(2):142–150.
15. Curley SA, Cherukuri P, Briggs K, et al. Noninvasive radiofrequency field-induced hyperthermic cytotoxicity in human cancer cells using cetuximab-targeted gold nanoparticles. *J Exp Ther Oncol.* 2008; 7(4):313–26. [PubMed: 19227011]
16. Kattumuri V, Katti K, Bhaskaran S, et al. Gum Arabic as a Phytochemical Construct for the Stabilization of Gold Nanoparticles: In Vivo Pharmacokinetics and X-ray-Contrast-Imaging Studies. *Small.* 2007; 3(2):333–341. [PubMed: 17262759]
17. Boisselier E, Astruc D. Gold nanoparticles in nanomedicine: preparations, imaging, diagnostics, therapies and toxicity. *Chemical Society Reviews.* 2009; 38(6):1759–1782. [PubMed: 19587967]
18. Kemp MM, et al. Gold and silver nanoparticles conjugated with heparin derivative possess anti-angiogenesis properties. *Nanotechnology.* 2009; 20(45):455104. [PubMed: 19822927]
19. Yang L, Wang H-J, Yang H-Y, et al. Shape-controlled synthesis of protein-conjugated silver sulfide nanocrystals and study on the inhibition of tumor cell viability. *Chemical Communications.* 2008; (26):2995–2997. [PubMed: 18688326]
20. Zhang F, Braun GB, Shi Y, et al. Fabrication of Ag@SiO₂@Y₂O₃:Er Nanostructures for Bioimaging: Tuning of the Upconversion Fluorescence with Silver Nanoparticles. *Journal of the American Chemical Society.* 132(9):2850–2851. [PubMed: 20158187]
21. Chompoosor A, Han G, Rotello VM. Charge Dependence of Ligand Release and Monolayer Stability of Gold Nanoparticles by Biogenic Thiols. *Bioconjugate Chemistry.* 2008; 19(7):1342–1345. [PubMed: 18553895]
22. El-Sayed IH, Huang X, El-Sayed MA. Selective laser photo-thermal therapy of epithelial carcinoma using anti-EGFR antibody conjugated gold nanoparticles. *Cancer letters.* 2006; 239(1): 129–135. [PubMed: 16198049]
23. Gannon C, Patra C, Bhattacharya R, Mukherjee P, Curley S. Intracellular gold nanoparticles enhance non-invasive radiofrequency thermal destruction of human gastrointestinal cancer cells. *Journal of Nanobiotechnology.* 2008; 6(1):2. [PubMed: 18234109]
24. Bhattacharya R, Mukherjee P. Biological properties of “naked” metal nanoparticles. *Advanced Drug Delivery Reviews Inorganic Nanoparticles in Drug Delivery.* 2008; 60(11):1289–1306.
25. Hong R, Fischer NO, Verma A, Goodman CM, Emrick T, Rotello VM. Control of Protein Structure and Function through Surface Recognition by Tailored Nanoparticle Scaffolds. *Journal of the American Chemical Society.* 2004; 126(3):739–743. [PubMed: 14733547]
26. Verma A, Uzun O, Hu Y, et al. Surface-structure-regulated cell-membrane penetration by monolayer-protected nanoparticles. *Nat Mater.* 2008; 7(7):588–595. [PubMed: 18500347]
27. You CC, Miranda OR, Gider B, Ghosh SP, Kim I, Erdogan B, Krovi SA, Bunz UHF, Rotello VM. Detection and identification of proteins using nanoparticle-fluorescent polymer ‘chemical nose’ sensors. *Nature Nanotechnology.* 2007; 2:318–323.
28. Patra CR, Bhattacharya R, Wang E, et al. Targeted delivery of gemcitabine to pancreatic adenocarcinoma using cetuximab as a targeting agent. *Cancer Res.* 2008; 68(6):1970–8. [PubMed: 18339879]
29. Folkman J. Angiogenesis. *Annu Rev Med.* 2006; 57:1–18. [PubMed: 16409133]
30. Bhattacharya R, Kang-Decker N, Hughes DA, et al. Regulatory role of dynamin-2 in VEGFR-2/KDR-mediated endothelial signaling. *Faseb J.* 2005; 19(12):1692–4. [PubMed: 16049137]
31. Bhattacharya R, Mukherjee P, Xiong Z, Atala A, Soker S, Mukhopadhyay D. Gold nanoparticles inhibit VEGF165-induced proliferation of HUVEC cells. *Nano Letters.* 2004; 4(12):2479–2481.
32. Pale-Grosdemange C, Simon ES, Prime KL, Whitesides GM. Formation of self-assembled monolayers by chemisorption of derivatives of oligo(ethylene glycol) of structure HS(CH₂)₁₁(OCH₂CH₂)mOH on gold. *Journal of the American Chemical Society.* 1991; 113(1): 12–20. 10.1021/ja00001a002
33. Zakrzewska M, Zhen Y, Wiedlocha A, Olsnes S, Wesche. Size Limitation in Translocation of Fibroblast Growth Factor 1 Fusion Proteins across the Endosomal Membrane. *Biochemistry.* 2009; 48(30):7209–7218. [PubMed: 19558187]

34. Wu C-SC, Thompson SA, Yang JT. Basic fibroblast growth factor is a β -rich protein. *Journal of Protein Chemistry*. 1991; 10(4):427–436. [PubMed: 1781888]
35. Nakaji-Hirabayashi T, Kato K, Iwata H. Surface-Anchoring of Spontaneously Dimerized Epidermal Growth Factor for Highly Selective Expansion of Neural Stem Cells. *Bioconjugate Chemistry*. 2008; 20(1):102–110. [PubMed: 19154156]
36. Miller K, Wang M, Gralow J, et al. Paclitaxel plus Bevacizumab versus Paclitaxel Alone for Metastatic Breast Cancer. *N Engl J Med*. 2007; 357(26):2666–2676. [PubMed: 18160686]
37. Campos S, Ghosh S. A Current Review of Targeted Therapeutics for Ovarian Cancer. *Journal of Oncology*. 2010; 2010:1–11.
38. Stone RL, Sood AK, Coleman RL. Collateral damage: toxic effects of targeted antiangiogenic therapies in ovarian cancer. *The Lancet Oncology*. 11(5):465–475. [PubMed: 20226736]
39. Ferrari M. Cancer nanotechnology: opportunities and challenges. *Nat Rev Cancer*. 2005; 5(3):161–71. [PubMed: 15738981]
40. Buckley RG, Elsome AM, Fricker SP, et al. Antitumor properties of some 2-[(dimethylamino)methyl]phenylgold(III) complexes. *J Med Chem*. 1996; 39(26):5208–14. [PubMed: 8978849]
41. Mukherjee P, Bhattacharya R, Wang P, et al. Antiangiogenic properties of gold nanoparticles. *Clin Cancer Res*. 2005; 11(9):3530–4. [PubMed: 15867256]
42. Mukherjee P, Bhattacharya R, Bone N, et al. Potential therapeutic application of gold nanoparticles in B-chronic lymphocytic leukemia (BCLL): enhancing apoptosis. *J Nanobiotechnology*. 2007; 5:4. [PubMed: 17488514]
43. Bhattacharya R, Patra CR, Earl A, et al. Attaching folic acid on gold nanoparticles using noncovalent interaction via different polyethylene glycol backbones and targeting of cancer cells. *Nanomed*. 2007; 3:224–238.
44. Goodman CM, McCusker CD, Yilmaz T, Rotello VM. Toxicity of gold nanoparticles functionalized with cationic and anionic side chains. *Bioconjug Chem*. 2004; 15:897–900. [PubMed: 15264879]
45. Verma A, Stellacci F. Effect of Surface Properties on Nanoparticle-Cell Interactions. *Small*. 2010; 6(1):12–21. [PubMed: 19844908]

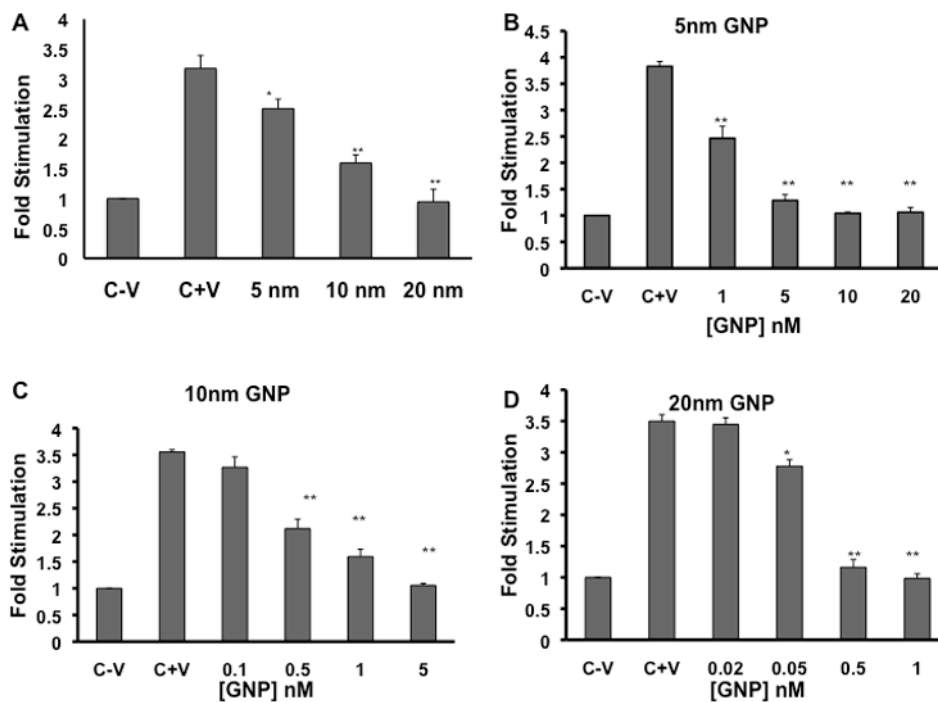


Figure 1. Effect of gold nanoparticle core size on cell proliferation in HUVECs [^3H] Thymidine incorporation is represented as fold stimulation. (A) Serum starved HUVECs were stimulated with 10 ng/ml VEGF165 that was preincubated with and without gold nanoparticles (conc = 1nmol/L) (B-D) The effect of dose on HUVEC proliferation with 5nm (B), 10nm (C), and 20nm GNPs (D). The analysis for each nanoparticle were done in triplicate and each C+V = cells stimulated with VEGF165 only. * = $P < 0.01$, ** = $P < 0.005$ as determined by a two-tailed student t-test. Error bars, mean \pm SD.

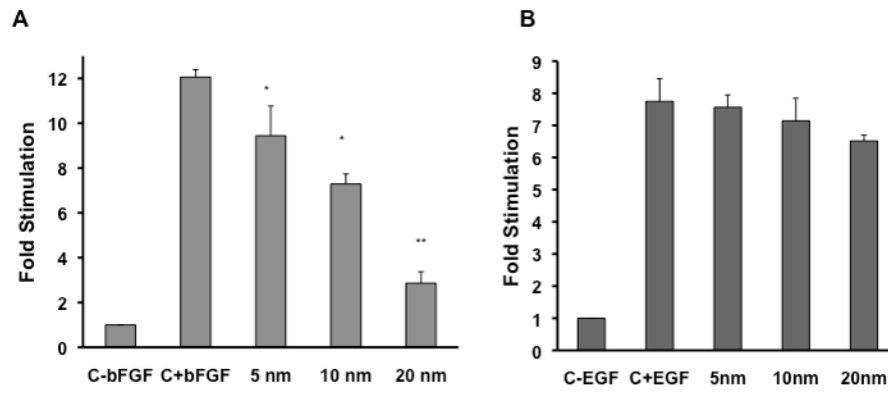


Figure 2. Effect of gold nanoparticle core size on cell proliferation in NIH3T3
 $[^3\text{H}]$ Thymidine incorporation is represented as fold stimulation. Serum starved NIH3T3 were stimulated with 10 ng/ml bFGF (A) or EGF (B) that was preincubated with and without gold nanoparticles (conc = 1 nmol/L). The analysis for each nanoparticle were done in triplicate and each experiment was repeated independently three times. c-b, c-e = only cells, c+b, c+e = cells stimulated with GF. * = $P < 0.01$, ** = $P < 0.005$ as determined by a two-tailed student t-test. Error bars, mean \pm SD.

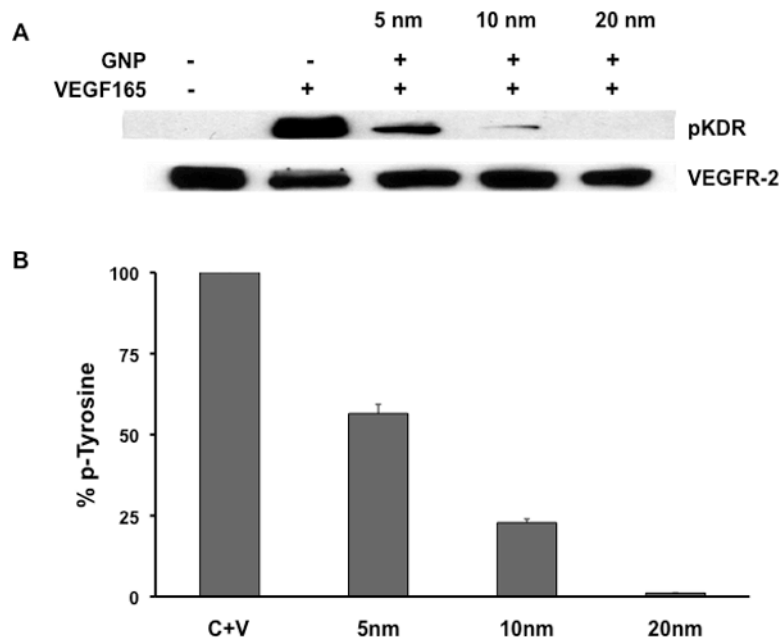


Figure 3. GNPs effect the phosphorylation of VEGF165 receptor

(A) Serum starved HUVECs were stimulated for 5 minutes with VEGF165 (10ng/mL) that was preincubated with or without gold nanoparticles and then immunoblotted with antibodies to phosphotyrosine KDR (pKDR) and total KDR levels in the cell extracts. (B) Densitometric scanning of phosphotyrosine blots using NIH Image, expressed in percentage. Experiments were performed in triplicate.

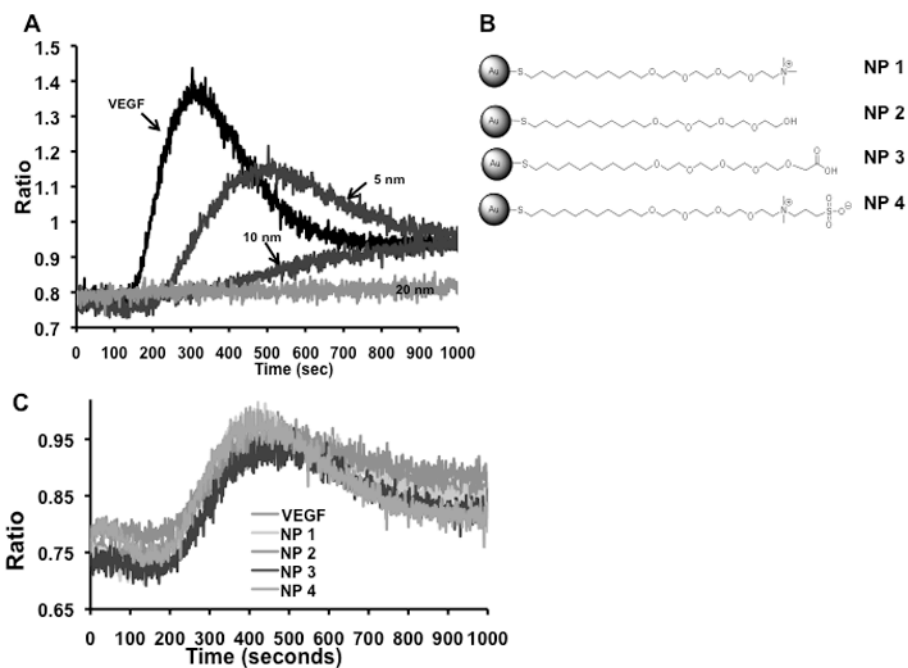


Figure 4. Response of calcium signaling in HUVECs in the presence of GNPs

Serum-starved HUVECs were suspended in Ca^{2+} buffer containing Fura-2AM dye and were stimulated with VEGF165 (10ng/mL) that was preincubated with or without gold nanoparticles. The top panel (A) shows the effect of surface size of GNPs on VEGF signaling cascade. (B) Schematic of the GNPs with different surface charges. In panel (C), VEGF165 was preincubated with charge modified GNPs. Experiments were performed in triplicates.

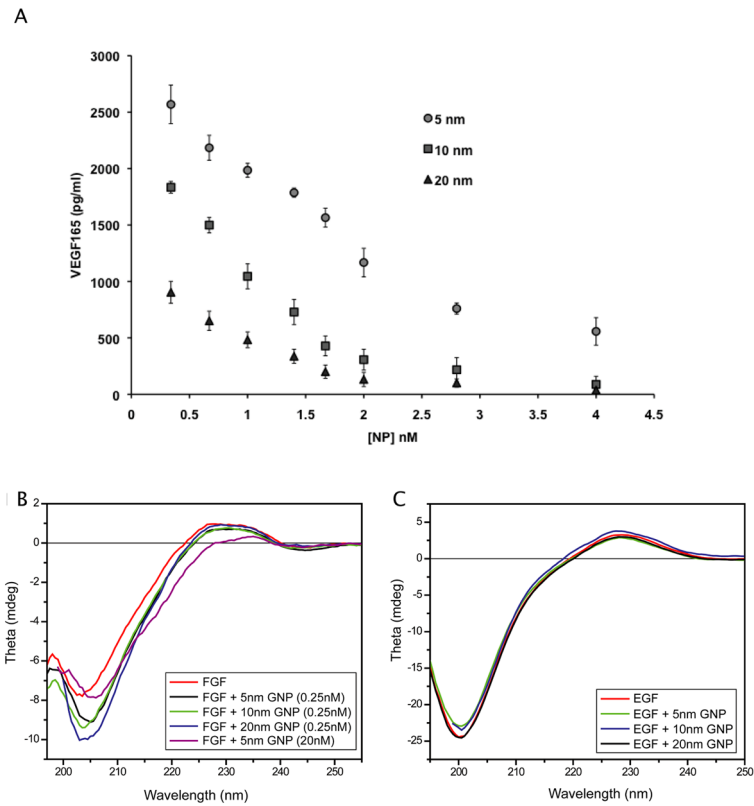


Figure 5. Affinity of VEGF165 binding is dependent on the surface size of GNP
 Gold nanoparticles (5nm, 10nm, and 20nm) were incubated with VEGF165. (A) An ELISA was used to quantify the amount of VEGF bound to the nanoparticle surface. Three independently performed experiments showed similar outcomes. Error bars, mean \pm SD. (B, C) Far UV-CD spectra was measured from 180 to 250 nm in a 1cm cuvette (B) 0.2mg/mL bFGF in were incubated with and without GNPs in 5mM phosphate buffer (C) 0.15 mg/mL EGF were incubated and without GNPs under similar conditions as listed above. The blanks containing GNPs with same concentration in buffer were subtracted from each data set